Sphingolipidomics of A2780 human ovarian carcinoma cells treated with synthetic retinoids

Manuela Valsecchi, Massimo Aureli, Laura Mauri, Giuditta Illuzzi, Vanna Chigorno, Alessandro Prinetti, and Sandro Sonnino[1]

Department of Medical Chemistry, Biochemistry and Biotechnology, Center of Excellence on Neurodegenerative Diseases, University of Milano, 20090 Segrate, Italy

Abstract The dihydroceramide, ceramide, sphingomyelin, lactosylceramide, and ganglioside species of A2780 human ovarian carcinoma cells treated with the synthetic retinoids *N*-(4-hydroxyphenyl)retinamide (fenretinide, 4-HPR) and 4-oxo-*N*-(4-hydroxyphenyl)retinamide (4-oxo-4-HPR) in culture were characterized by ESI-MS. We characterized 32 species of ceramide and dihydroceramide, 15 of sphingomyelin, 12 of lactosylceramide, 9 of ganglioside GM2, and 6 of ganglioside GM3 differing for the long-chain base and fatty acid structures. Our results indicated that treatment with both 4-HPR and 4-oxo-4-HPR led to a marked increase in dihydroceramide species, while only 4-oxo-4-HPR led to a minor increase of ceramide species. Dihydroceramides generated in A2780 cells in response to 4-HPR or 4-oxo-4-HPR differed for their fatty acid content, suggesting that the two drugs differentially affect the early steps of sphingolipid synthesis. Dihydroceramides produced upon treatments with the drugs were further used for the synthesis of complex dihydrosphingolipids, whose levels dramatically increased in drug-treated cells.—Valsecchi, M., M. Aureli, L. Mauri, G. Illuzzi, V. Chigorno, A. Prinetti, and S. Sonnino. **Sphingolipidomics of A2780 human ovarian carcinoma cells treated with synthetic retinoids. *J. Lipid Res.* 2010.** 51: **1832–1840.**

Supplementary key words 4-HPR • fenretinide • 4-oxo-4-HPR

The synthetic retinoid *N*-(4-hydroxyphenyl)retinamide (fenretinide, HPR) is cytotoxic in vitro to a variety of cancer cell types, including neuroblastoma, breast, lung, prostate, and ovarian. Together with these in vitro studies, several animal experimentations and preclinical or clinical studies suggest that fenretinide might represent a promising antitumor agent. In particular, in a phase III breast cancer prevention trial, it has proven to be effective in reducing the incidence of second breast malignancies in premenopausal women, with a concomitant reduction of ovarian cancer incidence (1). Currently, HPR is under clinical trials for the cure of prostatic and ovarian cancers, neuroblastoma, lymphoma, and leukemia. Many pieces of evidence indicate a link between HPR's antitumor effect and the metabolism of sphingolipids in tumor cells. As for many other anticancer drugs, the studies in tumor cell lines indicated that apoptosis is the major cytotoxic mechanism for HPR [even if the toxic effect of HPR is likely very complex and at least in part due to nonapoptotic mechanisms (2, 3)], and HPR-induced apoptosis in cancer cells has been ascribed to the increased cellular levels of ceramide, a sphingolipid mediator playing multiple roles in apoptotic signaling, elicited by HPR (4). The main metabolic mechanism responsible for HPR-induced production of ceramide is represented by de novo synthesis. Exposure to HPR of human neuroblastoma (5) and prostate cancer cells (6) resulted in a time- and dose-dependent increase in the activity of serine palmitoyltansferase and (dihydro)ceramide synthase, which catalyze early steps in the biosynthesis of ceramide and derived sphingolipids (7), and the treatment of cultured cells with pharmacological inhibitors of these enzymes was able to block HPR-induced ceramide increase (5, 6, 8). However, the effects of HPR on sphingolipid metabolism are probably much more complex and still poorly understood. For example, the possible role of sphingomyelin turnover due to the action of sphingomyelinases in the HPR-elicited ceramide production is still controversial, and conflicting results have been reported (8, 9). In neuroblastoma

This work was supported by grants from CARIPLO and AIRC to S.S.

Manuscript received 13 November 2009 and in revised form 25 February 2010.

Published, JLR Papers in Press, February 25, 2010
DOI 10.1194/jlr.M004010

Abbreviations: Cer, ceramide or dihydroceramide; ceramide, *N*-acyl-sphingosine; sphingosine, (2*S*,3*R*,4*E*)-2-amino-1,3-dihydroxy-octadecene, *d*18:1; *d*18:2, a sphingosine with a second double bond in unknown position within the hydrophobic chain; dihydroceramide, *N*-acyl-sphinganine; sphinganine. (2*S*,3*R*,)-2-amino-1,3-dihydroxy-octadecane, *d*18:0; long-chain base, *d*18:0, *d*18:1, or *d*18:0; lactosylceramide, LacCer, β-Gal-(1-4)-β-Glc-(1-1)-Cer; GM2, II^{3}Neu5AcGg$_3$Cer, β-GalNAc-(1-4)-[α-Neu5Ac-(2-3)-]β-Gal-(1-4)-β-Glc-(1-1)-Cer; GM3, II^{3}Neu5AcLacCer, α-Neu5Ac-(2-3)-β-Gal-(1-4)-β-Glc-(1-1)-Cer; 4-HPR, 4-[3,7-dimethyl-9-(2,6,6-trimethyl-1-cyclohexen-1-yl)-2,4,6,8-nonatetraenamido]-1-hydroxybenzene, *N*-(4-hydroxyphenyl)retinamide; 4-oxo-4-HPR, 4-oxo-*N*-(4-hydroxyphenyl)retinamide. Nomenclature of ceramide/dihydroceramide hydrophobic moiety: first sphingosine/sphinganine and then fatty acid.

[1]To whom correspondence should be addressed.
e-mail: sandro.sonnino@unimi.it

cells, HPR-induced ceramide production seems to be at least in part due to the activation of acidic sphingomyelinase, and a concomitant increase in the activity of glucosylceramide synthase and GD3 synthase with consequent accumulation of GD3, possibly responsible for HPR-induced apoptosis, was observed. Chronic treatment of human ovarian carcinoma cells with sublethal doses of HPR that led to the acquisition of a form of resistance to the drug was associated with a strong upregulation of GM3 synthase with consequent increased ganglioside levels (10). Moreover, MS analysis of sphingolipids from HPR-treated human neuroblastoma, prostate, and breast cancer cells revealed that dihydroceramide, and not ceramide, is accumulated upon HPR treatment with a concomitant increase in sphinganine, sphinganine-1-phosphate, and complex dihydrosphingolipids (dihydrosphingomyelin and monoexosyldihydroceramides) (7, 11, 12). The accumulation of dihydroceramides in HPR-treated cells is likely due to the increased de novo synthesis, mediated by the drug effect on serine palmitoyltansferase and/or (dihydro)ceramide synthase, with the concomitant inhibition of dihydroceramide desaturase, because the latter enzyme activity was strongly inhibited by HPR in intact cells and in a cell-free enzyme assay (7, 11). This effect has been probably neglected in the past studies reporting on HPR-induced ceramide elevation that relied mainly on TLC analysis for the detection of ceramide, not allowing the separation of saturated and unsaturated ceramide species. This raises the question whether HPR cytotoxicity is really linked to its effect on ceramide synthesis; many papers suggest that dihydroceramides are inactive on the pathways modulated by ceramides, but it has recently been reported that dihydroceramides can induce autophagy in prostate cancer cells (7) and cell growth inhibition with cell cycle arrest at G_0/G_1 in neuroblastoma cells (11). These findings emphasize the need for a better characterization of the effects of HPR on sphingolipid metabolism that imply the need for a wider application of lipidomics approaches.

MATERIALS AND METHODS

Materials

Commercial chemicals were the purest available. Sphingosine was prepared from cerebroside (13). Lyso-sphingomyelin was from Sigma-Aldrich. Lactosylsphingosine and lyso-gangliosides were prepared from the corresponding glycolipid (14). C17-sphingolipids were prepared by acylation of sphingosine or lyso-derivatives using heptadecanoic anhydride (15). 4-HPR was from Sigma, St. Louis, MO. 4-oxo-4-HPR was synthesized as previously described (16).

Cell cultures and cell treatments

A2780 human ovarian tumor cells (17) were cultured in RPMI 1640 (Sigma) supplemented with 10% of heat-inactivated FBS (GIBCO, Invitrogen, Carlsbad, CA), 2 mM glutamine, 100 units/ml penicillin, and 100 μg/ml streptomycin. Twenty-four hours after seeding, cells were treated with drugs for 48 h. 4-HPR and 4-oxo-4-HPR were dissolved at 10 mmol/L in DMSO and diluted to 10 μmol/L in culture medium immediately before use. Control cells were incubated with culture medium containing the same amount of DMSO as treated cells (0.1%).

Lipid extraction

Vehicle- and drug-treated cells were harvested and lyophilized, and cell lipids were extracted with chloroform/methanol 2:1 (v/v). The total lipid extract from each sample was subjected to a two-phase partitioning (10), resulting in the separation of an aqueous phase containing gangliosides and an organic phase containing all other lipids. The organic phase was submitted to alkaline treatment followed by partitioning to remove glycerophospholipids, and the alkali-treated organic phase was used for MS analysis.

MS

MS analyses were carried out using a Thermo Quest Finnigan LCQDeca ion trap mass spectrometer (FINNIGAN MAT, San Jose, CA) equipped with an ESI ion source and an Xcalibur data system and a TSP P4000 quaternary pump HPLC. Separations of all total sphingolipids were obtained on a 5 μm, 250 × 4mm LiChrospher 100 RP8 column (Merck).

Elution of sphingomyelin (SM) and Cer molecular species was carried out at a flow rate of 0.5 ml/min, with a gradient formed by the solvent system A, consisting of methanol/water (90:10 by vol), and solvent system B, consisting of methanol, both containing 5 mM ammonium acetate. The gradient elution program was as follows: 5 min with solvent A; 5 min with a linear gradient from 100% solvent A to 100% solvent B; 15 min with 100% solvent B; 5 min with a linear gradient from 100% solvent B to 100% methanol. Methanol was also used to wash the column for 10 min, followed by equilibration procedure with solvent A for 15 min.

Elution of ganglioside molecular species was carried out at a flow rate of 0.5 ml/min using a gradient formed by the solvent system A, consisting of CH_3CN/5 mM ammonium acetate buffer, pH7 (15:85 by volume), and solvent B containing CH_3CN/H_2O (85:15 by volume). The gradient was linear from 30:70 to 20:80, by volume, of A:B over 25 min, followed by a 5 min gradient from 20:80 to 0:100, by volume, of A:B, followed by 15 min of isocratic condition at 100% of B.

Elution of lactosylceramide molecular species was carried out at a flow rate of 1 ml/min, with a gradient formed by the solvent system A, consisting of methanol/water (90:10 by vol) containing 5 mM ammonium acetate, and solvent system B, consisting of methanol. The gradient elution program was as follows: 5 min with solvent A; 30 min with a linear gradient from 100% solvent A to 100% solvent B; 10 min with 100% solvent B.

Optimum conditions for SM and Cer molecular species MS analyses included sheath gas flow of 50 arbitrary units, spray voltage of 4 kV, capillary voltage of 47 V, capillary temperature of 260°C, and fragmentation voltage (used for collision-induced dissociation) of 40–60%. Mass spectra were acquired over a *m/z* range of 200–1000.

Optimum conditions for ganglioside molecular species MS analyses included sheath gas flow of 70 arbitrary units, auxiliary gas flow of 10 arbitrary units, spray voltage of 4 kV, capillary voltage of −42 V, capillary temperature of 260°C, and fragmentation voltage (used for collision induced dissociation) of 40–80%. Mass spectra were acquired over a range of *m/z* 200–2,000.

Optimum conditions for lactosylceramide molecular species MS analyses included sheath gas flow of 50 arbitrary units, spray voltage of 5 kV, capillary voltage of −15 V, capillary temperature of 260°C, and fragmentation voltage (used for collision induced dissociation) of 40–60%. Mass spectra were acquired over a *m/z* range of 200–1,500.

For all experiments, source ion optics were adjusted to accomplish desolvation of ions while minimizing fragmentation.

As internal standards, we used uncommon d18:1/17:0 sphingolipids (d18:1/17:0-Cer, d18:1/17:0-SM and d18:1/17:0-Lac-

Cer). A stock solution for each internal standard in ammonium acetate 5 mM in methanol was quantitatively prepared (50 μM) and stored at −20°C. Serial dilutions were prepared from these stock solutions and utilized for calibration curves.

Enzyme assays

3-Ketosphinganine synthase activity was performed as described previously (18). The final reaction volume of 0.1 ml contained 100 mM HEPES (pH 8.3), 2.5 mM EDTA, 5 mM dithiothreitol, 50 μM pyridoxal phosphate, 200 μM palmitoyl-CoA, 1 mM serine, and 0.01 [^{3}H]L-serine (specific radioactivity 26 Ci/mmol), and 300, 600, or 900 μg of total cell protein. The reactions were performed at three different incubation times: 10, 15, and 20 min. Control experiments were carried out on lysed cells maintained for 30 min at 90°C. At the end of the incubation time, radioactive 3-ketosphinganine was purified by partitioning the total lipid extract (19); radioactive 3-ketosphinganine was detected by TLC separation. Dihydroceramide desaturase activity was performed as described previously (18). The final reaction volume of 0.3 ml contained 100 mM sodium phosphate buffer (pH 7.4), 3 mM NADH, 15 nmol of dihydroceramide and 0.1 nmol of [^{3}H]dihydroceramide (specific radioactivity 1.36 Ci/mmol), and 600–1,200 μg of total cell protein. The substrate solubilizations were performed using CHAPS and BSA systems (20). After 60–120 min, the reactions were terminated and lipids were extracted by phase partitioning as previously described (20). Radioactive ceramide and dihydroceramide were detected

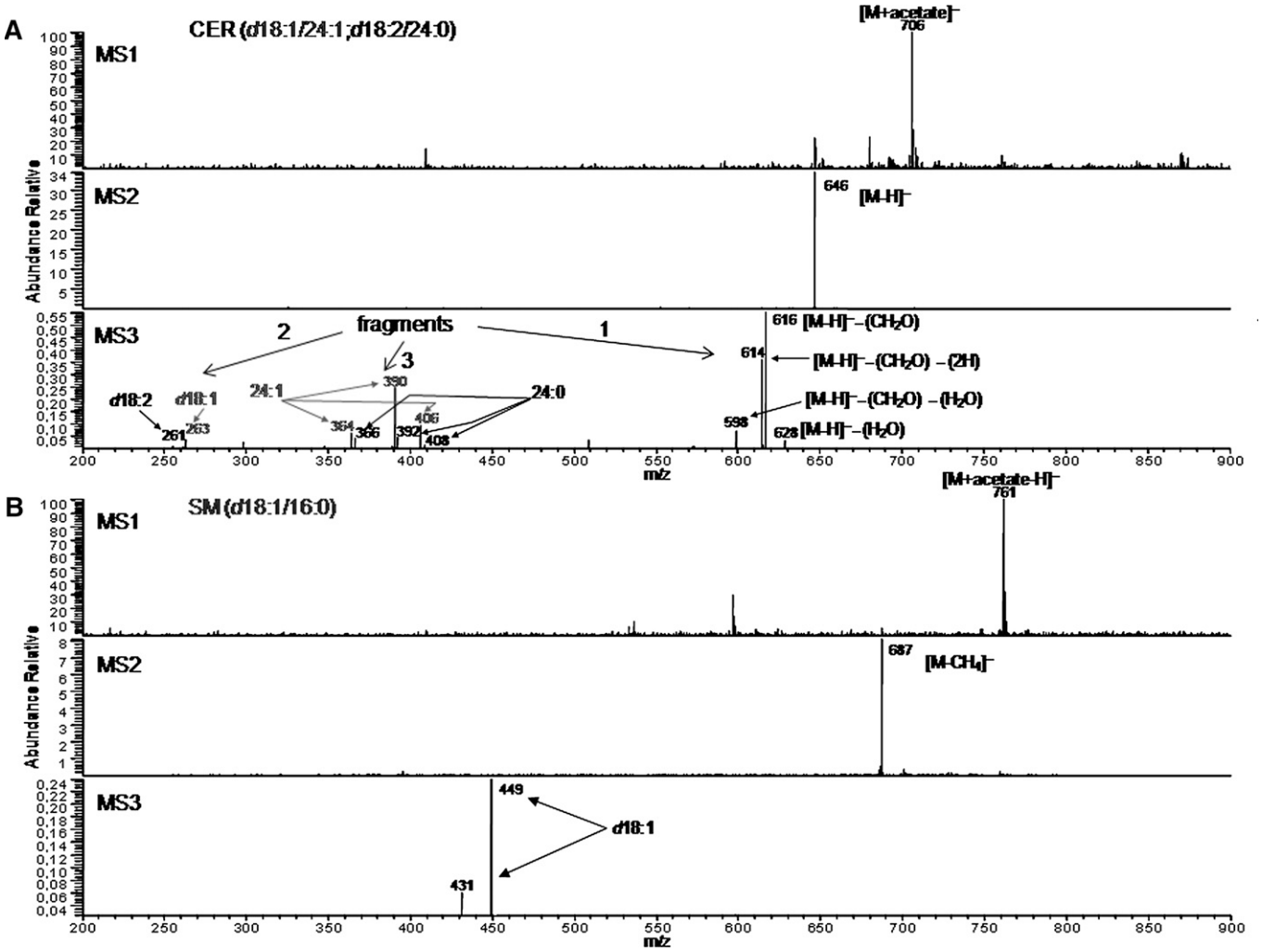

Fig. 1. MS characterization of sphingolipids species from A2780 cells. A: Characterization of the acetate-adduct ion at *m/z* 706 corresponding to a Cer species containing *d*18:1/24:1 or *d*18:2/24:0. Figure shows the MS1 spectrum, the MS2 spectrum derived from the acetate-adduct ion at *m/z* 706, and the MS3 spectrum derived from the molecular ion at *m/z* 646. In MS2 analysis, collision activation of this [M + CH3COO] adduct ion yielded essentially the deprotonated molecular ion, and its fragmentation yielded many abundant product ions, each containing salient structural information. In MS3 analysis, the collision induced dissociation (CID) pattern of deprotonated ceramide ions was constituted by fragment ions that can be classified into three groups: 1) fragments formed by loss of small neutrals, 2) fragments referring to the long chain base structure, and 3) fragments referring to the acyl structure. This pattern is consistent with the possible pathway proposed by others authors (31, 32). The conclusion is that the ion at 706 corresponds to both *d*18:1/24:1 and *d*18:2/24:0 that were not separated by HPLC connected to the MS. B: Characterization of the ion at 761 corresponding to SM(*d*18:1/16:0) or SM(*d*18:0/16:1). MS1 spectrum of sphingomyelin, in the negative ion mode, was dominated by molecular ion adduct with acetate. MS2 spectrum derived from the acetate-adduct ion at *m/z* 761 gave a product ion due to loss of acetate and methyl group of phosphocoline headgroup. MS3 spectrum derived from the [M-CH_4] ion at *m/z* 687 gave a product ion due to loss of fatty acid moiety. These product ions are characteristic of the sphingoid base, and their *m/z* reveals the number of carbon atoms in the chain, degree of hydroxylation, unsaturation, or other structural modifications of the base. The conclusion is that the analyzed ion correspond to SM(*d*18:1/16:0).

by TLC separation. Dihydroceramide synthase activity was performed as described previously (21). The final reaction volume of 0.1 ml contained 50 mM HEPES (pH 7.5), 0.5 mM dithiothreitol, 5 μM sphingosine, 0.1 μM of [1-^{3}H]sphingosine (specific radioactivity 1.36 Ci/mmol) contained in 1 μl of ethanol, and 400–800 μg of total cell proteins. As acyl-CoA substrate, we used 25 μM of palmitoyl-CoA, stearoyl-CoA, and lignoceroyl-CoA; in the case of lignoceroyl-CoA, 0.1% of digitonin was added (22). After 15–30 min, the reactions were terminated and lipids were extracted by the addition of chloroform/methanol (2:1 by volume). Radioactive ceramide and sphingosine were detected by TLC separation. For all the procedures, radioactive lipid detection was performed by digital autoradiography analysis (Betaimager Biospace,). Thus, the product formed was calculated on the basis of the TLC radioactivity percent distribution (analysis was performed by Betavision software). There were three sets of experiments, each one performed in triplicate.

Other analytical methods

The protein content was determined on cell homogenates according to Lowry (23) using BSA as reference standard. Experiments were run in triplicate unless otherwise stated. Data are expressed as mean value ± SD and were analyzed by one-way ANOVA followed by the Student-Neuman-Keuls' test. *P*-values are indicated in the legend of each figure.

RESULTS AND DISCUSSION

In this paper, we report on the sphingolipid composition of the A2780 human ovarian carcinoma cell line under basal conditions or upon treatment with two synthetic retinoids, 4-HPR and 4-oxo-4-HPR (24, 25), potentially useful as therapeutic agents in a variety of tumors. Our sphingolipidomic analysis encompassed dihydroceramide and ceramide species as well sphingomyelin and glycosphingolipid (gangliosides and LacCer) species.

Like many other antitumor drugs, 4-HPR exerts its cytotoxic action at least in part through an apoptotic mechanism, which was reported to be triggered by the drug-elicited increase in the levels of the pro-apoptotic sphingolipid ceramide (4). It was proposed that the main mechanism responsible for ceramide generation upon treatment with 4-HPR was represented by the de novo biosynthesis (5, 6, 25). Indeed, 4-HPR was shown to activate serine palmitoyltansferase and dihydroceramide synthase, which catalyze the early steps in the biosynthesis of ceramide (5); in addition, it has been shown more recently that 4-HPR stimulation of ceramide de novo biosynthesis is accompanied by the concomitant inhibition of dihydroceramide desatu-

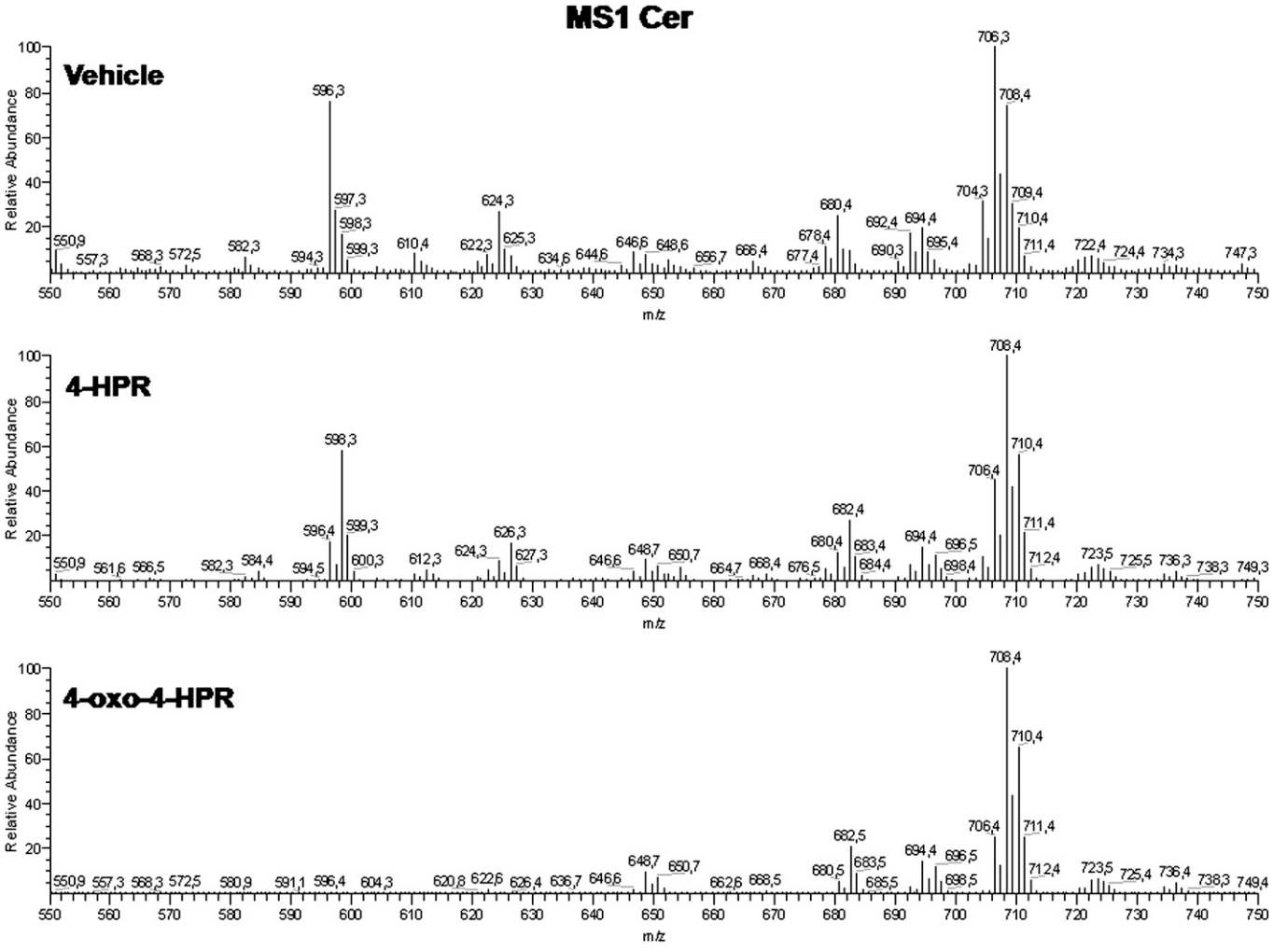

Fig. 2. Mass spectra of the total Cer mixtures from A2780, 4-HPR, and 4-oxo-4-HPR A2780 treated cells. The fragmentation patterns for Cer species are presented in a previous report (28).

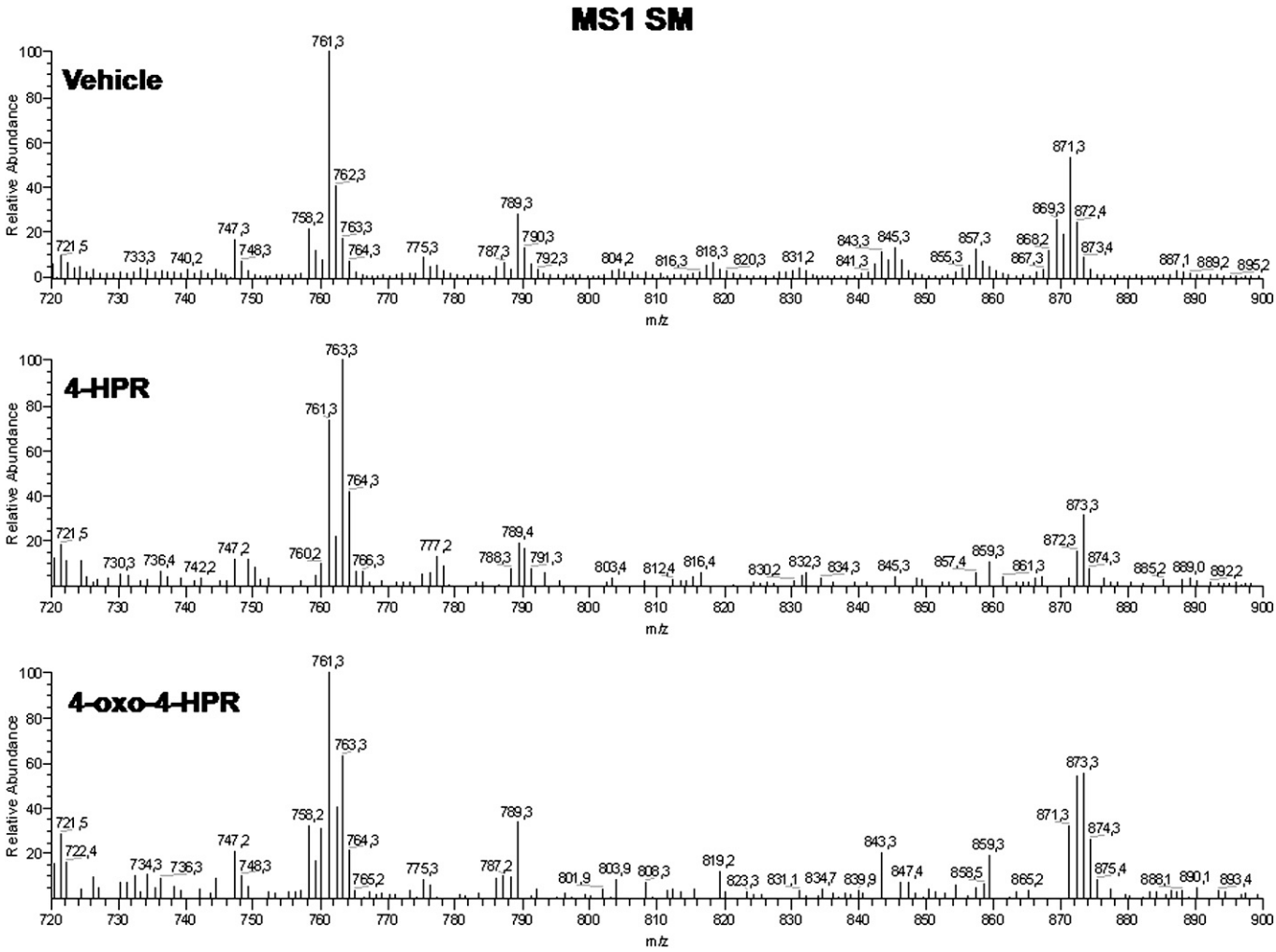

Fig. 3. Mass spectra of the total sphingomyelin mixtures from A2780, 4-HPR, and 4-oxo-4-HPR treated A2780 cells. The fragmentation patterns for SM species are presented in a previous paper (28).

rase (7, 11), thus resulting in the accumulation of dihydroceramide, rather than ceramide, as confirmed by MS analysis of sphingolipids from 4-HPR-treated tumor cells of different origin (7, 12, 26, 27). We analyzed the activity of serine palmitoyltansferase, ceramide synthase, and dihydroceramide desaturase, and in agreement with the previous information (5, 7, 11), we found that under our experimental conditions 4-HPR treatment activated serine palmitoyltansferase 81 ± 13%, activated ceramide synthase 40 ± 9% and 48 ± 9%, using C16 and C24 fatty acids, respectively, while it inhibited dihydroceramide deasaturase 85 ± 8%.

This represents a clear example of the importance of sphingolipidomics in elucidating the exact role of specific molecular species in sphingolipid-mediated biological and pharmacological events.

In this work, we used MS to determine the complex sphingolipid species pattern of control and drug-treated A2780 cells. We analyzed dihydroceramide, ceramide, sphingomyelin, lactosylceramide, GM2 ganglioside, and GM3 ganglioside species, which together cover the majority of complex lipids. Examples of mass spectra are reported in **Figs. 1–3** and data on the pattern of each sphingolipid family are reported in Figs. 4–8. The molecular species differing in the lipid moiety of Cer (here and elsewhere, Cer is used to identified all the ceramide and dihydroceramide species), SM, LacCer, and gangliosides were characterized by identification of the ions obtained

TABLE 1. Sphingolipid content in control and drug-treated A2780 cells

	Cer	SM	LacCer	GM3	GM2	Total Sphingolipid
Control	0.73 ± 0.05	13.21 ± 0.39	1.98 ± 0.19	0.29 ± 0.03	1.39 ± 0.14	17.60 ± 0.80
10 μM 4-HPR	3.46 ± 0.18*	14.44 ± 0.28	2.42 ± 0.22*	0.18 ± 0.02	0.86 ± 0.12	21.36 ± 0.82
10 μM 4-oxo-4-HPR	2.86 ± 0.17*	11.45 ± 0.46	3.36 ± 0.27*	0.50 ± 0.04	1.46 ± 0.13	19.63 ± 1.07

Data are expressed as nmol/mg protein and are the means of three different experiments. *$P < 0.01$.

by MS1, MS2, and MS3. Quantitative data referred to different quantities of synthetic sphingolipids containing *d*18:1 sphingosine and 17:0 fatty acid added to the samples as reference standards. A linear correlation between a series of solutions of these compounds and the ion peak intensities was obtained by multiple reactions monitoring analysis, as shown in a previous report (28).

In agreement with previous results, analysis of Cer from control and 4-HPR-treated A2780 cells revealed that treatment with 10 μM 4-HPR for 48 h was able to induce a 4.7-fold increase in total Cer level (**Table 1**); this was mainly due to an increase of dihydroceramide species (**Fig. 4**). Dihydroceramide species were present in a faint amount in control cells, while they accounted for 2.89 nmol/mg protein of the 3.46 nmol/mg protein of Cer in 4-HPR-treated cells (**Table 2**). This corresponded to about a 40-fold increase of dihydroceramides in 4-HPR-treated cells versus controls. The *d*18:1 ceramide level was substantially unchanged (539 pmol/mg protein and 545 pmol/mg protein in control and 4-HPR-treated cells, respectively) (Table 2), and *d*18:2 ceramide species were present as minor components in both control and treated cells.

4-Oxo-4-HPR, a recently identified metabolite of 4-HPR (16), showed a similar but not identical effect on Cer content in A2780 cells. It caused a marked increase in dihydroceramide, even if less pronounced with respect to 4-HPR (25-fold vs. control cells). Our enzymatic studies support the notion that 4-oxo-4-HPR is an effective inhibitor of dihydroceramide desaturase, as 4-HPR. 4-Oxo-4-HPR inhibited dihydroceramide dehydrogenase 82 ± 15%, and this supports and explains the high increase of dihydroceramide with respect of ceramide. On the other hand, treatment with 4-oxo-4-HPR was also able to induce a small but significant increase in the level of *d*18:1 ceramides

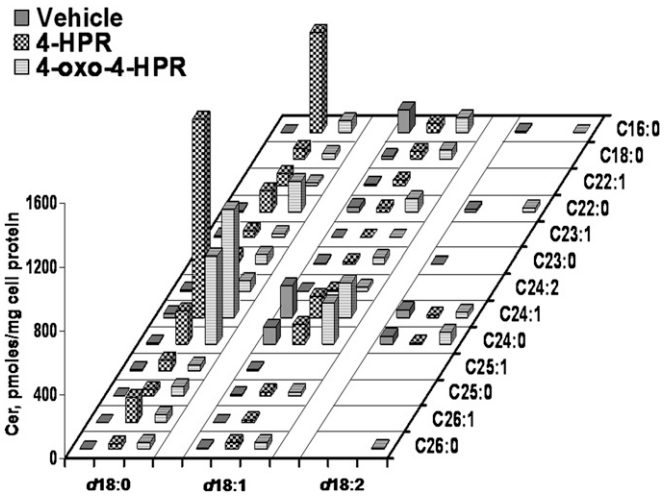

Fig. 4. Cer species in A2780, 4-HPR treated A2780, and 4-oxo-4-HPR A2780 treated cells, as determined by MS. The X axis reports the long-chain base content of sphinganine, sphingosine, or sphingosine with a second double bond in an unknown position; the Y axis reports the content of each fatty acid species. Data are expressed as pmol/mg cell protein and are the means of three different experiments, with SD never exceeding 15% of the mean values.

TABLE 2. Dihydroceramide and ceramide content in control and drug-treated A2780 cells

	Total	*d*18:0	*d*18:1
Control	0.73 ± 0.05	0.07 ± 0.01	0.54 ± 0.04
10 μM 4-HPR	3.46 ± 0.18*	2.89 ± 0.15*	0.54 ± 0.03
10 μM 4-oxo-4-HPR	2.86 ± 0.17*	1.86 ± 0.11*	0.86 ± 0.06*

Data are expressed as nmol/mg protein and are the means of three different experiments. *$P < 0.01$.

(+60% vs. controls). This is in agreement with the previous information suggesting that 4-oxo-4-HPR is able, as 4-HPR, to stimulate the de novo synthesis of Cer (25). However, the relative potency of 4-HPR and 4-oxo-4-HPR on serine palmitoyltansferase/ceramide synthase is likely different, given the different response elicited in term of sphingolipid species by the two drugs. This is in part confirmed by the enzymatic results. 4-Oxo-4-HPR treatment activated serine palmitoyltansferase 79 ± 14%, a value overlapping that determined with 4-HPR, while activating ceramide synthase 20 ± 6% and 33 ± 9%, using C16 and C24 fatty acids, respectively, against 40 ± 9% and 48 ± 9% using 4-HPR.

This is as highlighted by the results presented in Fig. 4. Cer production upon treatment with 4-HPR and 4-oxo-4-HPR was selective for different molecular species, not only on the basis of their sphingosine/sphinganine content, but also on the basis of the fatty acid content, with respect to the fatty acyl chain length and the presence of unsaturations. Basically, all dihydroceramide species were increased upon treatment with 4-HPR and 4-oxo-4-HPR; however, the contribution of different molecular species to the total increase was dramatically different within the same treatment and between the two drugs. In 4-HPR-treated cells, the main Cer species were *d*18:0/24:1 and *d*18:0/16:0 (accounting together for about 65% of total dihydroceramides in these cells), while in 4-oxo-4-HPR-treated cells, the main species were *d*18:0/24:1 and *d*18:0/24:0 (about 65% of total dihydroceramides): *d*18:0/24:0 and *d*18:0/16:0 represented only 7.1% and 4.0% of total dihydroceramides in 4-HPR and 4-oxo-4-HPR-treated cells, respectively. Collectively, the ratio between C16 and C24 fatty acyl chain-containing dihydroceramide species was about 7-fold higher in 4-HPR than in 4-oxo-4-HPR-treated cells. Within molecular species with the same acyl chain length, C24:0/C24:1, C22:0/C22:1, and C26:0/C26:1 ratios were 5-, 7-, and 3-fold higher, respectively, in 4-oxo-4-HPR-treated than in 4-HPR-treated cells (**Table 3**). It can be speculated that these differences could originate from a different availability of fatty acyl-CoA substrated for dihydroceramide synthesis (but no evidence so far can support this hypothesis) or from a different effect of on different Cer synthases. Six different genes for Cer synthases are cur-

TABLE 3. Ratios between dihydroceramide species with different acyl chain length and unsaturation in 4-HPR and 4-oxo-4-HPR-treated cells

	C16/C24	C24:0/C24:1	C22:0/C22:1	C26:0/C26:1
4-HPR	0.40	0.17	1.75	0.23
4-oxo-4-HPR	0.06	0.80	11.62	0.80

rently known, and each enzyme is characterized by a substrate selectivity for fatty acyl-CoA with different chain lengths (7, 29). It should be noted that in many cases the enzyme selectivity assignments are still tentative, and no information is available for selectivity toward fatty acyl-CoA with different degrees of desaturation. On the basis of the current knowledge, it is tempting to speculate that 4-HPR is a relatively more potent activator of CerS-5/6, the main one responsible for the synthesis of C16-containing dihydroceramides, and 4-oxo-4-HPR more effectively affect CerS-2/3, selective for C24 fatty acyl-CoA.

Because Cer is the backbone for the synthesis of more complex sphingolipids, not surprisingly, the extensive remodeling of Cer species that occurred in A2780 cells upon treatment with 4-HPR and 4-oxo-4-HPR had profound consequences on the patterns of sphingomyelin and glycosphingolipid species.

In the case of sphingomyelin (**Fig. 5**), the main molecular species in untreated cells were those with *d*18:1/16:0 and *d*18:1/24:1 (61% and 18% of total SM, respectively). The corresponding species containing dihydroceramide were absent or present as minor compounds. Drug treatment did not significantly affect total SM levels (Table 1). However, upon treatment with 4-HPR and, to a lesser extent with 4-oxo-4-HPR, species with ceramide dramatically decreased while those species with dihydroceramide proportionally increased (Fig. 5), without a consistent remodeling of the fatty acid composition (even if the C16/C24 ratio was slightly higher in SM from 4-HPR-treted cells, 4.5 vs. 3.0 in controls). Thus, the SM species with 16:0 containing dihydroceramide became the main species of 4-HPR-treated cells (42.5% on total species).

GM3 and GM2 are the main gangliosides in A2780 cells. **Figure 6** shows that in the case of gangliosides, the main species in untreated cells was that with *d*18:1/16:0 ceramide for both GM3 and GM2. Gangliosides containing sphinganine were detectable as minor compounds. Treatment with 4-HPR and, less pronouncedly, with 4-oxo-4-HPR, caused a significant increase of the species with sphinganine. However, the species with sphingosine also remained the most abundant in drug-treated cells (Fig. 6).

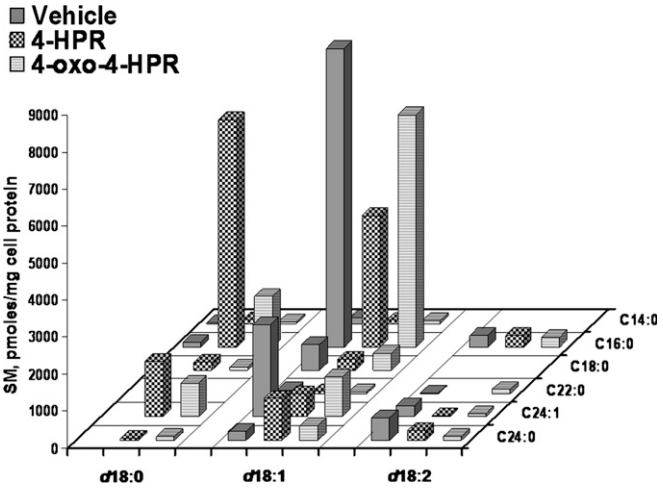

Fig. 5. Sphingomyelin species in A2780, 4-HPR treated A2780, and 4-oxo-4-HPR A2780 treated cells, as determined by MS. X axis reports the long-chain base content of sphinganine, sphingosine or sphingosine with a second double bond in an unknown position; the Y axis reports the content of each fatty acid species. Data are expressed as pmol/mg cell protein and are the means of three different experiments, with SD never exceeding 15% of the mean values.

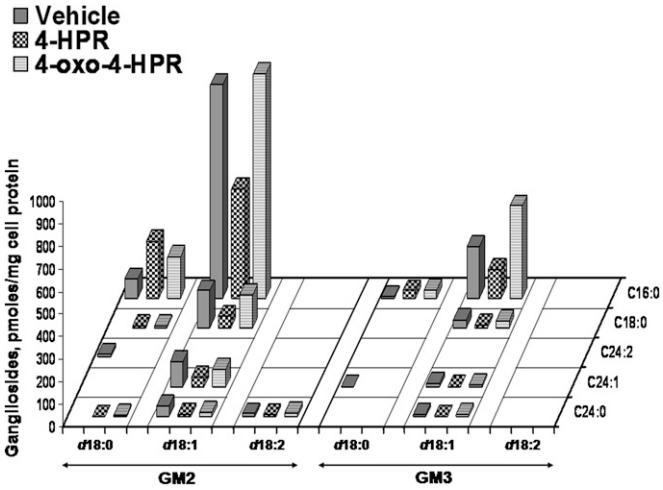

Fig. 6. GM2 and GM3 ganglioside species in A2780, 4-HPR treated A278,0 and 4-oxo-4-HPR A2780 treated cells, as determined by MS. X axis reports the long-chain base content of sphinganine, sphingosine or sphingosine with a second double bond in an unknown position; the Y axis reports the content of each fatty acid species. Data are expressed as pmol/mg cell protein and are the means of three different experiments, with SD never exceeding 15% of the mean values.

Figure 7 shows data for LacCer. In A2780 cells, the main species of LacCer was that with *d*18:1/16:0 followed by that with *d*18:1/24:1. However, the species with 24:1 dihydroceramide was not neglectable. Treatment with 4-HPR and, more pronouncedly, with 4-oxo-4-HPR caused a significant increase of the species with dihydroceramides, particularly those with palmitic acid. Treatment with 4-oxo-4-HPR caused an increase of LacCer.

Together, our data on sphingolipidomics of A2780 cells under basal conditions or upon treatment with 4-HPR or 4-oxo-4-HPR allow some comments. Treatment with both retinoids led to an increase in dihydroceramides with changes in Cer total cell content; the fatty acid profile of Cer was different in cells treated with 4-HPR or 4-oxo-4-HPR and controls, suggesting that the two drugs differentially affect the pathway leading to Cer generation. This finding could explain the different sensitivity of various tumor cell lines to the two drugs (24) and could contribute to define strategies allowing to overcome the resistance to 4-HPR treatment. The elevation in dihydroceramides rather than ceramides is in agreement with data obtained in breast and colon carcinoma and leukemia cells (12). Because dihydroceramides are usually not considered proapoptotic mediators but have been involved as possible triggers for autophagic cell death (7), these data might indicate that the mechanism of 4-HPR-induced cell death is even more complex than thought. De novo synthesized dihydroceramides are further used for the synthesis of

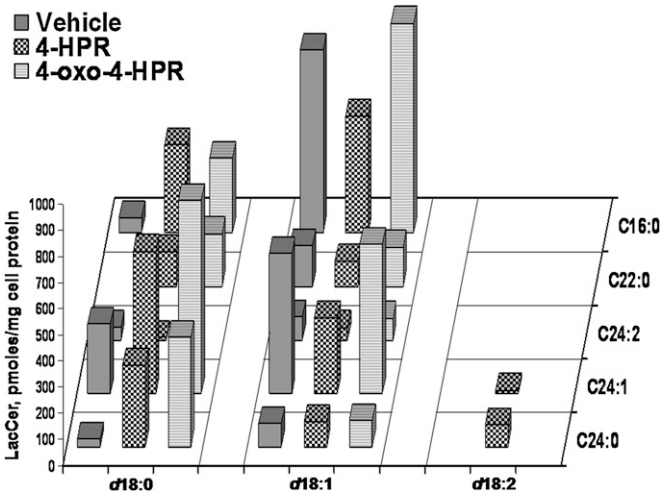

Fig. 7. Lactosylceramide species in A2780, 4-HPR treated A2780, and 4-oxo-4-HPR A2780 treated cells, as determined by MS. The X axis reports the long-chain base content of sphinganine, sphingosine or sphingosine with a second double bond in unknown position; the Y axis reports the content of each fatty acid species. Data are expressed as pmol/mg cell protein, and are the means of three different experiments with SD never exceeding 15% of the mean values.

complex dihydrosphingolipids, including dihydrosphingomyelin, dihydrogangliosides, and dihydrolactosylceramide, usually present in cells (including A2780) in a faint amount. Increase in dihydrosphingolipids occurred at different degrees for the different sphingolipid classes and for the two drugs, but was dramatic. Drug treatments produced changes in the content of each sphingolipid family but no large changes in the total cell sphingolipid content; this suggests that the total quantity of biosynthesized Cer necessary to have cell Cer species and Cer as precursor of the cell complex sphingolipids does not change too much but that the different Cer structures containing sphingosine or sphinganine and a fatty acid displaying different length and degree of unsaturation are capable to address the following biosynthetic pathway determining the synthesis of a specific group of complex sphingolipids, sphingomyelin, gangliosides, or neutral glycolipids.

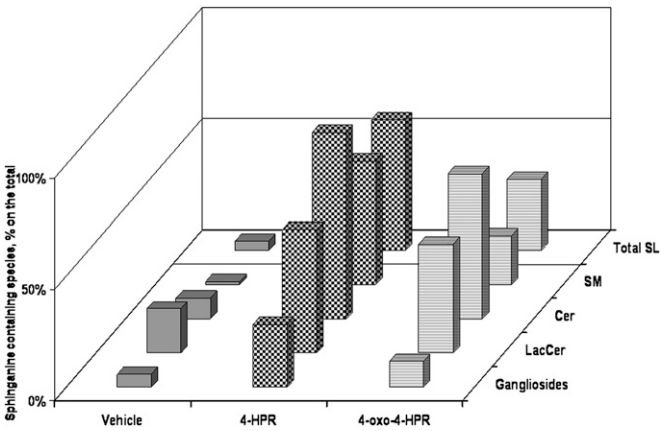

Fig. 8. Percentage content, on the total, of the species of ganglioside, lactosylceramide, cer, sphingomyelin, and total sphingolipids containing sphinganine in of A2780, 4-HPR treated A2780, and 4-oxo-4-HPR A2780 treated cells. The figure has been prepared from data reported in Figures 4–7.

Given these results, it is reasonable to wonder whether the anomalously high levels of dihydrosphingolipids, about 58.8% and 31.9% on the total (see **Fig. 8**) after 4-HPR and 4-oxo-4-HPR treatment, respectively, might somehow contribute to the drug effect. It can be easily predicted, for instance, that vesicular sphingolipid intracellular traffic and the lateral organization of sphingolipids in lipid rafts (thought to regulate several aspects of cell function, including pathways influencing cell proliferation and survival) (30) will be deeply altered in retinoid-treated A2780 cells.

These results are a clear example of the new perspectives that can be opened in an even intensely explored field by the structure-specific and quantitative information obtained through a sphingolipidomic approach.

REFERENCES

1. Bonanni, B., M. Lazzeroni, and U. Veronesi. 2007. Synthetic retinoid fenretinide in breast cancer chemoprevention. *Expert Rev. Anticancer Ther.* **7:** 423–432.
2. Tiwari, M., V. K. Bajpai, A. A. Sahasrabuddhe, A. Kumar, R. A. Sinha, S. Behari, and M. M. Godbole. 2008. Inhibition of N-(4-hydroxyphenyl) retinamide-induced autophagy at a lower dose enhances cell death in malignant glioma cells. *Carcinogenesis.* **29:** 600–609.
3. Tosetti, F., R. Vene, G. Arena, M. Morini, S. Minghelli, D. M. Noonan, and A. Albini. 2003. N-(4-hydroxyphenyl)retinamide inhibits retinoblastoma growth through reactive oxygen species-mediated cell death. *Mol. Pharmacol.* **63:** 565–573.
4. Hail, N., Jr., H. J. Kim, and R. Lotan. 2006. Mechanisms of fenretinide-induced apoptosis. *Apoptosis.* **11:** 1677–1694.
5. Wang, H., B. J. Maurer, C. P. Reynolds, and M. C. Cabot. 2001. N-(4-hydroxyphenyl)retinamide elevates ceramide in neuroblastoma cell lines by coordinate activation of serine palmitoyltransferase and ceramide synthase. *Cancer Res.* **61:** 5102–5105.
6. Wang, H., A. G. Charles, A. J. Frankel, and M. C. Cabot. 2003. Increasing intracellular ceramide: an approach that enhances the cytotoxic response in prostate cancer cells. *Urology.* **61:** 1047–1052.
7. Zheng, W., J. Kollmeyer, H. Symolon, A. Momin, E. Munter, E. Wang, S. Kelly, J. C. Allegood, Y. Liu, Q. Peng, et al. 2006. Ceramides and other bioactive sphingolipid backbones in health and disease: lipidomic analysis, metabolism and roles in membrane structure, dynamics, signaling and autophagy. *Biochim. Biophys. Acta.* **1758:** 1864–1884.
8. Erdreich-Epstein, A., L. B. Tran, N. N. Bowman, H. Wang, M. C. Cabot, D. L. Durden, J. Vlckova, C. P. Reynolds, M. F. Stins, S. Groshen, et al. 2002. Ceramide signaling in fenretinide-induced endothelial cell apoptosis. *J. Biol. Chem.* **277:** 49531–49537.
9. Lovat, P. E., M. Corazzari, F. Di Sano, M. Piacentini, and C. P. Redfern. 2005. The role of gangliosides in fenretinide-induced apoptosis of neuroblastoma. *Cancer Lett.* **228:** 105–110.
10. Prinetti, A., L. Basso, V. Appierto, M. G. Villani, M. Valsecchi, N. Loberto, S. Prioni, V. Chigorno, E. Cavadini, F. Formelli, et al. 2003. Altered sphingolipid metabolism in N-(4-hydroxyphenyl)-retinamide-resistant A2780 human ovarian carcinoma cells. *J. Biol. Chem.* **278:** 5574–5583.
11. Kraveka, J. M., L. Li, Z. M. Szulc, J. Bielawski, B. Ogretmen, Y. A. Hannun, L. M. Obeid, and A. Bielawska. 2007. Involvement of dihydroceramide desaturase in cell cycle progression in human neuroblastoma cells. *J. Biol. Chem.* **282:** 16718–16728.
12. Wang, H., B. J. Maurer, Y. Y. Liu, E. Wang, J. C. Allegood, S. Kelly, H. Symolon, Y. Liu, A. H. Merrill, Jr., V. Gouaze-Andersson, et al. 2008. N-(4-hydroxyphenyl)retinamide increases dihydroceramide and synergizes with dimethylsphingosine to enhance cancer cell killing. *Mol. Cancer Ther.* **7:** 2967–2976.
13. Carter, H. E., J. A. Rothfus, and R. Gigg. 1961. Biochemistry of the sphingolipids: XII. Conversion of cerebrosides to ceramides and sphingosine; structure of Gaucher cerebroside. *J. Lipid Res.* **2:** 228–234.
14. Valiente, O., L. Mauri, R. Casellato, L. E. Fernandez, and S. Sonnino. 2001. Preparation of deacetyl-, lyso-, and deacetyl-lyso-

GM(3) by selective alkaline hydrolysis of GM3 ganglioside. *J. Lipid Res.* **42:** 1318–1324.
15. Palestini, P., M. Allietta, S. Sonnino, G. Tettamanti, T. E. Thompson, and T. W. Tillack. 1995. Gel phase preference of ganglioside GM1 at low concentration in two-component, two-phase phosphatidylcholine bilayers depends upon the ceramide moiety. *Biochim. Biophys. Acta.* **1235:** 221–230.
16. Villani, M. G., V. Appierto, E. Cavadini, M. Valsecchi, S. Sonnino, R. W. Curley, and F. Formelli. 2004. Identification of the fenretinide metabolite 4-oxo-fenretinide present in human plasma and formed in human ovarian carcinoma cells through induction of cytochrome P450 26A1. *Clin. Cancer Res.* **10:** 6265–6275.
17. Appierto, V., E. Cavadini, R. Pergolizzi, L. Cleris, R. Lotan, S. Canevari, and F. Formelli. 2001. Decrease in drug accumulation and in tumour aggressiveness marker expression in a fenretinide-induced resistant ovarian tumour cell line. *Br. J. Cancer.* **84:** 1528–1534.
18. Merrill, A., and Y. Hannun. 1999. Sphingolipid metabolism and cell signaling. *Methods Enzymol.* **311:** 3–30.
19. Williams, R. D., E. Wang, and A. H. Merrill, Jr. 1984. Enzymology of long-chain base synthesis by liver: characterization of serine palmitoyltransferase in rat liver microsomes. *Arch. Biochem. Biophys.* **228:** 282–291.
20. Michel, C., G. van Echten-Deckert, J. Rother, K. Sandhoff, E. Wang, and A. H. Merrill, Jr. 1997. Characterization of ceramide synthesis. A dihydroceramide desaturase introduces the 4,5-trans-double bond of sphingosine at the level of dihydroceramide. *J. Biol. Chem.* **272:** 22432–22437.
21. Mizutani, Y., A. Kihara, and Y. Igarashi. 2006. LASS3 (longevity assurance homologue 3) is a mainly testis-specific (dihydro)ceramide synthase with relatively broad substrate specificity. *Biochem. J.* **398:** 531–538.
22. Lahiri, S., H. Lee, J. Mesicek, Z. Fuks, A. Haimovitz-Friedman, R. N. Kolesnick, and A. H. Futerman. 2007. Kinetic characterization of mammalian ceramide synthases: determination of K(m) values towards sphinganine. *FEBS Lett.* **581:** 5289–5294.
23. Lowry, O. H., N. J. Rosebrough, A. L. Farr, and R. J. Randall. 1951. Protein measurement with the folin phenol reagent. *J. Biol. Chem.* **193:** 265–275.
24. Bonanni, B., and M. Lazzeroni. 2009. Retinoids and breast cancer prevention. *Recent Results Cancer Res.* **181:** 77–82.
25. Villani, M. G., V. Appierto, E. Cavadini, A. Bettiga, A. Prinetti, M. Clagett-Dame, R. W. Curley, and F. Formelli. 2006. 4-oxo-fenretinide, a recently identified fenretinide metabolite, induces marked G2-M cell cycle arrest and apoptosis in fenretinide-sensitive and fenretinide-resistant cell lines. *Cancer Res.* **66:** 3238–3247.
26. Merrill, A. H., Jr., T. H. Stokes, A. Momin, H. Park, B. J. Portz, S. Kelly, E. Wang, M. C. Sullards, and M. D. Wang. 2009. Sphingolipidomics: a valuable tool for understanding the roles of sphingolipids in biology and disease. *J. Lipid Res.* **50 (Suppl.):** S97–S102.
27. Schulz, T. J., R. Thierbach, A. Voigt, G. Drewes, B. Mietzner, P. Steinberg, A. F. Pfeiffer, and M. Ristow. 2006. Induction of oxidative metabolism by mitochondrial frataxin inhibits cancer growth: Otto Warburg revisited. *J. Biol. Chem.* **281:** 977–981.
28. Valsecchi, M., L. Mauri, R. Casellato, S. Prioni, N. Loberto, A. Prinetti, V. Chigorno, and S. Sonnino. 2007. Ceramide and sphingomyelin species of fibroblasts and neurons in culture. *J. Lipid Res.* **48:** 417–424.
29. Pewzner-Jung, Y., S. Ben-Dor, and A. H. Futerman. 2006. When do Lasses (longevity assurance genes) become CerS (ceramide synthases)?: insights into the regulation of ceramide synthesis. *J. Biol. Chem.* **281:** 25001–25005.
30. Prinetti, A., N. Loberto, V. Chigorno, and S. Sonnino. 2009. Glycosphingolipid behaviour in complex membranes. *Biochim. Biophys. Acta.* **1788:** 184–193.
31. Raith, K., and R. H. H. Neubert. 1998. Structural studies on ceramides by electrospray tandem mass spectrometry. *Rapid Commun. Mass Spectrom.* **12:** 935–938.
32. Raith, K., and R. H. H. Neubert. 2000. Liquid chromatography-electrospray mass spectrometry and tandem mass spectrometry of ceramides. *Anal. Chim. Acta.* **403:** 295–303.